The Journal of Immunology

Associations of Simian Immunodeficiency Virus (SIV)-Specific Follicular CD8 $^{+}$ T Cells with Other Follicular T Cells Suggest Complex Contributions to SIV Viremia Control

Mohammad Arif Rahman, Katherine M. McKinnon, Tatiana S. Karpova, David A. Ball, David J. Venzon, Wenjin Fan, Guobin Kang, Qingsheng Li and Marjorie Robert-Guroff

J Immunol published online 5 March 2018
http://www.jimmunol.org/content/early/2018/03/03/jimmunol.1701403

The Journal of Immunology is published twice each month by
The American Association of Immunologists, Inc.,
1451 Rockville Pike, Suite 650, Rockville, MD 20852

Print ISSN: 0022-1767 Online ISSN: 1550-6606.

Published March 5, 2018, doi:10.4049/jimmunol.1701403

Associations of Simian Immunodeficiency Virus (SIV)-Specific Follicular CD8$^+$ T Cells with Other Follicular T Cells Suggest Complex Contributions to SIV Viremia Control

Mohammad Arif Rahman,* Katherine M. McKinnon,* Tatiana S. Karpova,† David A. Ball,† David J. Venzon,‡ Wenjin Fan,§ Guobin Kang,§ Qingsheng Li,§ and Marjorie Robert-Guroff*

Follicular CD8$^+$ T (fCD8) cells reside within B cell follicles and are thought to be immune-privileged sites of HIV/SIV infection. We have observed comparable levels of fCD8 cells between chronically SIV-infected rhesus macaques with low viral loads (LVL) and high viral loads (HVL), raising the question concerning their contribution to viremia control. In this study, we sought to clarify the role of SIV-specific fCD8 cells in lymph nodes during the course of SIV infection in rhesus macaques. We observed that fCD8 cells, T follicular helper (Tfh) cells, and T follicular regulatory cells (Tfreg) were all elevated in chronic SIV infection. fCD8 cells of LVL animals tended to express more Gag-specific granzyme B and exhibited significantly greater killing than did HVL animals, and their cell frequencies were negatively correlated with viremia, suggesting a role in viremia control. Env- and Gag-specific IL-21$^+$ Tfh of LVL but not HVL macaques negatively correlated with viral load, suggesting better provision of T cell help to fCD8 cells. Tfreg positively correlated with fCD8 cells in LVL animals and negatively correlated with viremia, suggesting a potential benefit of Tfreg via suppression of chronic inflammation. In contrast, in HVL macaques, Tfreg and fCD8 cell frequencies tended to be negatively correlated, and a positive correlation was seen between Tfreg number and viremia, suggesting possible dysfunction and suppression of an effective fCD8 cell immune response. Our data suggest that control of virus-infected cells in B cell follicles not only depends on fCD8 cell cytotoxicity but also on complex fCD8 cell associations with Tfh cells and Tfreg. ***The Journal of Immunology*****, 2018, 200: 000–000.**

Among the earliest manifestations of the epidemic disease that came to be known as AIDS was persistent, generalized lymphadenopathy, first seen in homosexual males (1, 2). Lymph node (LN) follicles were subsequently identified as important sites of replication and trapping of the etiologic agent of the disease, HIV (3, 4), as well as of SIV in the rhesus macaque model (5). Subsequently, CD4$^+$ Th cells in LN follicles, now known as T follicular helper (Tfh) cells (6, 7), were identified as key targets of both HIV (8–10) and SIV infection (11, 12) in secondary lymphoid tissue.

During HIV infection, Tfh cells in B cell follicles produce HIV and are responsible for persistent virus transcription in long-term aviremic individuals treated with antiretroviral therapy (ART) (13). Significantly higher concentrations of SIV-producing cells have been reported to occur in B cell follicles compared with extrafollicular regions of the spleen, LN, and gut-associated lymphoid tissue of SIV-infected macaques during chronic asymptomatic infection (14). Furthermore, residual SIV infection has been localized in B cell follicles of rhesus macaques undergoing fully suppressive ART (15). Such observations have suggested that germinal center (GC) Tfh cells comprise an immune-privileged site for HIV/SIV replication (14, 16, 17), which may not be readily accessible to ART or to antiviral CD8$^+$ T cells that lack expression of the follicular homing molecule, CXCR5. Thus, the production of HIV/SIV in GC Tfh cells represents a major obstacle to obtaining a functional cure for HIV/SIV infection.

In HIV infection, CD8$^+$ T cells, especially Gag-specific CTL (18, 19), play a role in control of viral load. Early studies showed that depletion of CD8$^+$ T cells in SIV-infected animals impaired viremia control (20, 21). Furthermore, cytotoxic CD8$^+$ T cells were detected in LN GC of HIV-infected individuals (22, 23), as well as in LNs of SIV-infected nonhuman primates (24, 25). However, LNs, among other tissues, have come to be considered sanctuaries where reservoirs of Tfh cells infected with HIV or SIV can persist (15, 26). The observation that tetramer$^+$CD8$^+$ T cells, although present in extrafollicular areas of LNs of HIV-infected subjects were mostly absent in follicles, provided a rationale for the persistence of HIV/SIV in lymphoid Tfh cells (16). The growing focus of the field on obtaining an HIV cure, requiring elimination of viral reservoirs, has stimulated new studies on quantitation and functional capability of CD8$^+$ T cells in lymphoid follicles.

In healthy humans, a subset of CD8$^+$ T cells was reported to use CXCR5 to enter B cell follicles (27). CXCR5$^+$CD8$^+$ T cells,

*Vaccine Branch, Center for Cancer Research, National Cancer Institute, National Institutes of Health, Bethesda, MD 20892; †Center for Cancer Research Core Fluorescence Imaging Facility, Laboratory of Receptor Biology and Gene Expression, National Cancer Institute, National Institutes of Health, Bethesda, MD 20892; ‡Biostatistics and Data Management Section, National Cancer Institute, National Institutes of Health, Bethesda, MD 20892; and §Nebraska Center for Virology, School of Biological Sciences, University of Nebraska–Lincoln, Lincoln, NE 68588

ORCIDs: 0000-0002-6120-8943 (M.A.R.); 0000-0003-4101-4073 (Q.L.).

Received for publication October 6, 2017. Accepted for publication February 7, 2018.

This work was supported by the Intramural Research Program of the National Institutes of Health, National Cancer Institute.

Address correspondence and reprint requests to Dr. Marjorie Robert-Guroff, National Cancer Institute, National Institutes of Health, 41 Medlars Drive, MSC5065, Building 41, Room D804, Bethesda, MD 20892-5065. E-mail address: guroffm@mail.nih.gov

Abbreviations used in this article: ART, antiretroviral therapy; fCD8, follicular CD8$^+$ T; GC, germinal center; HVL, high viral load; LCMV, lymphocytic choriomeningitis virus; LN, lymph node; LVL, low viral load; MFI, mean fluorescence intensity; RT, room temperature; Tfh, T follicular helper; Tfreg, T follicular regulatory cell; Treg, T regulatory cell.

termed follicular cytotoxic T cells, were subsequently identified in the lymphocytic choriomeningitis virus (LCMV) mouse model and shown to enter B cell follicles and eradicate LCMV-infected Tfh cells and B cells infected with the herpesvirus, MuHV-4 (28). $CXCR5^+CD8^+$ T cells were also reported to express lower levels of inhibitory receptors than the $CXCR5^-$ subset and exhibited more potent cytotoxicity against chronic LCMV infection (29). With regard to HIV/SIV infection, $CD8^+$ T cells with follicular cytotoxic T cell characteristics, including potential cytotoxic function, have been identified in lymphoid follicles. $CXCR5^+$ $CD8^+$ T cells in individuals infected with HIV were shown to correlate inversely with viral load (29). Granzyme B^+ CM-9-tetramer$^+$ (SIV Gag-specific) $CD8^+$ T cells in lymphoid follicles of mucosal tissue were enriched in chronically SIV-infected macaques that controlled infection compared with noncontrollers, and correlated inversely with lymphoid Tfh cells (30). Similarly, $CXCR5^+CD8^+$ T cells (termed follicular $CD8^+$ T [fCD8] cells) were increased in LN follicles and GC of HIV-infected individuals, and they exhibited expression of both granzyme B and perforin. In the presence of anti-HIV/anti-CD3 bispecific Ab these cells exhibited better killing in vitro compared with non-fCD8 cells (31). Overall, these reports substantiate that fCD8 cells are located in B cell follicles of secondary lymphoid tissue, the site of active HIV/SIV replication, and that they might be key contributors to viremia control.

In this study, we sought to clarify the role of viral-specific fCD8 cells during the course of SIV infection in rhesus macaques. Although previous studies have suggested that fCD8 cells might contribute to viremia control in chronic viral infections, they are observed in chronically SIV-infected macaques exhibiting high viral loads (HVL). This raises the question of whether fCD8 cells in HVL animals are functional. Furthermore, the interactions of other cell populations in B cell follicles and their effect on fCD8 cells have not been fully explored. In this study, we show that in low viral load (LVL) animals, fCD8 cells are associated with viremia control whereas associations of Tfh cells with fCD8 cells suggest provision of help through secretion of IL-21. In contrast, in HVL animals Tfh cells apparently fail to provide adequate help, T follicular regulatory cells (Tfreg) are associated with diminished fCD8 cells and increased viremia, and fCD8 cells overall are not correlated with a protective outcome.

Materials and Methods

Study animals and sample collection

Rhesus macaques (27 females, 24 males) were maintained at Advanced Bioscience Laboratories (Rockville, MD) and at the National Cancer Institute animal facility (Bethesda, MD) under the guidelines of the Association for the Assessment and Accreditation of Laboratory Animal Care and according to the recommendations of the *Guide for the Care and Use of Laboratory Animals*. Protocols and procedures were approved by the Institutional Animal Care and Use Committee of the respective facility. Inguinal LN biopsy specimens were collected from: 1) 12 naive macaques (includes preimmunization/infection samples from 4 of the acute group and 1 each from the LVL and HVL groups with no apparent clustering in the paired values); 2) 15 acutely infected macaques (samples obtained within 9–16 d of infection with SIV_{mac251}), for which 12 samples were used for flow cytometry and 5 were used in killing and ELISPOT assays; and 3) 24 chronically infected macaques (samples obtained 40–50 wk after SIV_{mac251} infection). These were previously vaccinated with replicating adenovirus–SIV recombinants and boosted with SIV gp120 or gp140 as described (32), or with either ALVAC–SIV recombinant plus SIV gp120 protein or SIV DNA plasmid plus gp120 protein (T.A. Musich, S. Helmold Hait, V. Mohanram, I. Tuero, E. Huiting, T. Hoang, R. Hunegnaw, Z. Mushtaq, L. Miller-Novak, M.A. Rahman, T. Demberg, A. Valentin, D.A. Vargas-Inchaustegui, D.J. Venzon, G. Franchini, B.K. Felber, G.N. Pavlakis, and M. Robert-Guroff, manuscript in preparation). They were divided into LVL (11 macaques) and HVL (13 macaques) groups. One macaque each in the LVL and HVL groups had received empty Ad vector and adjuvant only. Samples from 11 of each group were used for flow cytometry, and 5 from each group were used in killing and ELISPOT assays. Median plasma viral loads during week 12 until necropsy for LVL and HVL animals were $<3 \times 10^4$ and $>7 \times 10^4$ SIV RNA copies per milliliter of plasma, respectively. Geometric means of the median values for the HVL and LVL macaques were 1.20×10^6 and 1.86×10^3, respectively. CD4 counts were not performed as routinely as the viral loads; however, median CD4 counts from the week 12 set point onward ranged from 641 to 923 for LVL macaques and from 248 to 552 for the HVL macaques. The means of the median CD4 counts for this time period were 805 and 384 for the LVL and HVL macaques, respectively. For LN viral loads, LN cells were lysed using QIAzol lysis reagent (Qiagen) and stored at −70°C until RNA extraction and viral load determination by droplet digital PCR as previously described (33). Fig. 1 illustrates the viral loads (Fig. 1A–C), CD4 counts (Fig. 1D–F), and LN viral loads (Fig. 1G) of macaques in the LVL and HVL groups. LN viral loads were directly correlated with both the median plasma viral loads during chronic infection (Fig. 1H) as well as with plasma viral loads at the time of LN collection (Fig. 1I). This is consistent with a previous report that significantly correlated plasma viral loads with SIV^+ follicular cells assessed by in situ hybridization (14). None of the macaques was diagnosed with clinical AIDS.

LN biopsies were minced and passed through a 40-μm cell strainer after lysis of RBCs. Cells were washed and resuspended in R10 (RPMI 1640 containing 10% FBS, 2 mM L-glutamine, 1% nonessential amino acids, 1% sodium pyruvate, and antibiotics). Cells were viably frozen in FBS plus 10% DMSO and thawed for all assays. Additional LN biopsies from three naive, five acute, four LVL, and five HVL animals were collected in OCT (Sakura Finetek, Torrance, CA) and frozen in liquid nitrogen for immunohistochemical analysis.

Flow cytometric detection of fCD8 cells, Tfh cells, and Tfreg

LN cells were stained with Aqua Live/Dead viability dye (Invitrogen, Carlsbad, CA) at room temperature (RT) for 15 min in PBS, washed with FACS wash, and surface stained with the following anti-human fluorochrome-conjugated mAbs cross-reactive with rhesus macaque Ags: Alexa Fluor 700 anti-CD3 (SP34-2), Brilliant Violet 650 anti-CD8 (RPA-T8), Brilliant Violet 711 anti-CD4 (L200), and PE-Cy7 anti-CD28 (CD28.2) from BD Biosciences (San Jose, CA); PE-Cy5 anti-CD95 (DX2) and allophycocyanin–eFluor 780 anti-CCR7 (3D12) from eBioscience (San Diego, CA); Brilliant Violet 786 anti-CD25 (BC96) and Brilliant Violet 605 anti–PD-1 (EH12.2H7) from BioLegend (San Diego, CA); and PE anti-CXCR5 (710D82.1) from the National Institutes of Health Nonhuman Primate Reagent Resource (Boston, MA). For detection of Tfreg, after surface staining cells were permeabilized with Foxp3/transcription factor staining buffer (eBioscience) and stained intracellularly with PerCP-Cy5.5 anti-Foxp3 (236A/E7) (BD Biosciences). At least 500,000 singlet events were acquired on a SORP LSR II (BD Biosciences) and analyzed using FlowJo software (FlowJo, Ashland, OR). For all samples, gating was established using a combination of isotype and fluorescence-minus-one controls.

Cytokine staining of SIV-specific Tfh and fCD8 cells

SIV-specific production of granzyme B, perforin, and IL-21 by LN-resident fCD8 and Tfh cells was assayed by stimulating LN cells in the presence of 2 μg/ml anti-CD49d and PE-Cy7 anti-CD28 (CD28.2) (BD Biosciences), BD GolgiPlug, BD GolgiStop, and allophycocyanin–eFluor 780 anti-CCR7 (3D12) at the manufacturer's recommended concentrations. One million cells were stimulated with pooled peptides spanning the SIV_{mac239} Gag (125 peptides) or Env (218 peptides) protein. Peptides were 15-mers overlapping by 11, with each peptide at 1 μg/ml (National Institutes of Health AIDS Research and Reference Reagent Program). Following incubation for 6 h at 37°C in 5% CO_2, cells were stained with Live/Dead Aqua dye followed by surface staining and permeabilization with Foxp3/transcription factor staining buffer. Intracellular staining was performed with Alexa Fluor 647 anti–IL-21 (3A3-N2.1) (BD Biosciences), FITC anti-perforin (Pf-344) (Mabtech, Cincinnati, OH), and PE–Texas Red anti–granzyme B (GB11) (Invitrogen/Life Technologies). Acquisition and analysis were as described above. SIV_{mac239} Gag- or Env-specific granzyme B, perforin, and IL-21 responses were calculated by subtracting the percentage unstimulated response from the percentage peptide-stimulated response. Specific mean fluorescence intensity (MFI) was calculated as the peptide-stimulated response minus the unstimulated response.

Cell sorting

LN cells from acutely and chronically infected animals were stained with Brilliant Violet 711 anti-CD4 (L200), FITC anti-CD8 (RPA-T8) (BD

Biosciences), and PE anti-CXCR5 (710D82.1) (National Institutes of Health Nonhuman Primate Reagent Resource). Aqua Live/Dead viability dye was used to exclude dead cells. After staining, cells were washed, passed through a 40-μm cell strainer, and sorted on an Astrios EQ flow cytometer. Three groups of live cells were sorted ($CD8^+CXCR5^-$, $CD8^+CXCR5^+$, and $CD4^+$) with purity of >85%.

ELISPOT assay

The ELISPOT assay was conducted using monkey IFN-γ ELISpot^{PLUS} (HRP) kits. The 96-well polyvinylidene plates were precoated with anti–IFN-γ mAb (mAb MT126L). After washing and blocking the plates, $CD8^+CXCR5^-$ or $CD8^+CXCR5^+$ sorted LN cells were serially diluted and plated in duplicate at 1×10^5, 0.5×10^5, and 0.25×10^5 cells per well. Cells were stimulated by adding either SIV_{mac239} Env or Gag pooled peptides (1 μg/ml each peptide) and incubating for 20 h at 37°C. Subsequently, plates were washed with PBS before the addition of biotinylated anti–IFN-γ mAb (7-B6-1) at 1 μg/ml. Following incubation at RT for 120 min, plates were washed with PBS and incubated with the manufacturer's recommended dilution of streptavidin-conjugated HRP for 60 min at RT. Following washes with PBS, spots resulting from individual IFN-γ–producing cells were visualized after a 15-min reaction with tetramethylbenzidine ready-to-use substrate solution, counted with an Eliphoto counter (CTL analyzer), and recorded per 10^6 $CD8^+$ T cells. As negative controls, cells were plated without peptide. SIV-specific spots were calculated by subtracting spots resulting from unstimulated cells.

Killing assay

Cytotoxic activity of $CD8^+$ T cells was assayed using a modified flow cytometry–based killing assay (34). Sorted autologous $CD4^+$ T cells, used as targets, were fluorescently labeled according to the manufacturer's recommendation with the CellTrace Violet dye kit (Thermo Fisher Scientific/Life Technologies, Grand Island, NY). The labeled $CD4^+$ cells were washed and pulsed with SIV_{mac239} Gag pooled peptides (1 μg/ml each peptide) for an hour. A portion of the cells was not peptide pulsed and served as control. Target cells (with/without peptide pulsing) were washed twice and 10,000 cells per well were plated in R10 in U-bottom 96-well plates. Effector $CD8^+CXCR5^-$ or $CD8^+CXCR5^+$ sorted LN cells were placed in different wells at 25:1 E:T ratios to a final volume of 200 μl. Plates were incubated at 37°C for 5 h. After incubation, cells were labeled by adding 0.25 μl of yellow Live/Dead viability dye (Invitrogen) in 100 μl of PBS per well. Plates were washed twice with PBS and cells were resuspended in 200 μl of 2% PBS–paraformaldehyde solution, transferred to acquisition tubes, and read on an LSR II. Killing was measured by incorporation of the yellow Live/Dead viability dye in CellTrace Violet$^+$ target cells. Specific killing was defined as percentage killing of peptide pulsed targets minus percentage killing of targets without peptide pulsing.

Immunohistochemical detection of GCs and GC-resident fCD8 and Tfh cells

Adjacent LN sections were stained for Tfh and fCD8 cells, respectively. Briefly, 6-μm sections were cut, adhered to salinized slides, and pretreated in 1 mM EDTA (pH 8) in a Presto pressure cooker (National Presto Industries, Eau Claire, WI) at 121°C for 35 s to unmask Ags. Sections were blocked with normal horse serum and incubated overnight at 4°C with the following primary Abs: rabbit monoclonal anti-human CD4 (clone EPR6855, catalog no. ab133616, 1:200; Abcam) or mouse monoclonal anti-human CD8 (clone RPA-T8, catalog no. 557084, 1:200; BD Biosciences), goat anti-human PD-1 (AF1086, 1:40; R&D Systems), and mouse monoclonal anti-human Ki67 (clone MM1, catalog no. VP-K452, 1:200; Vector Laboratories) for CD4 and PD-1 staining combination or rabbit monoclonal anti-human Ki67 (clone EPR3610, catalog no. ab92742, 1:200; Abcam) for CD8 and PD-1 staining combination. After washing in PBS, slides were incubated at RT for 2 h with the following secondary Abs for CD4 staining: AlexaFluor 594 donkey anti-rabbit IgG, AlexaFluor 488 donkey anti-goat IgG and AlexaFluor 647 donkey anti-mouse IgG and counterstained with DAPI. For CD8 staining secondary Abs included AlexaFluor 647 donkey anti-mouse IgG, AlexaFluor 488 donkey anti-goat IgG and AlexaFluor 594 donkey anti-rabbit IgG with DAPI counterstaining. The secondary Abs (diluted 1:200) were from Life Technologies. After washing in PBS, slides were coverslipped and examined. Images were collected on an LSM 780 confocal microscope with Zen software (Carl Zeiss, Thornwood, NY) using Plan-Apochromat ×40, 1.40 numerical aperture Zeiss objective and gallium arsenide phosphide detector. Panels of single focal plane images were acquired with pixel size of 415 or 519 nm at 12-bit image depth with averaging (setting 2) and pixel dwell time of 1.58 μs in the following channels: magenta (excitation, 633 nm; emission, 650–758), red (excitation, 561 nm; emission, 570–694 nm), green (excitation, 488 nm; emission, 490–553 nm), and blue (excitation, 405 nm; emission, 410–470 nm). For publication, images were scaled to 8-bit RGB identically, with a linear LUT and exported in the TIFF format. Figures were made from TIFF images in Adobe Illustrator without any change in resolution. Scale bars are provided for each image.

Quantification of GC-resident fCD8 and Tfh cells in fixed LNs

Ki67 staining defined GCs, as both light and dark zones have a high cell proliferation rate (35). The total area of individual GCs was determined by abundance of Ki67 and PD-1. The quantification of fCD8 and $CD4^+$ Tfh cells in GCs was performed as described (36). Cells expressing CD4 or CD8 were extracted from the entire confocal images by first using the interactive segmentation software ilastik (v1.1.5) (37) to separate cells from the background based on features defined by color/intensity, edges, and texture in all image channels. Although the ilastik segmentation efficiently delineated cells from the image background, groups of cells were not adequately separated from each other. Therefore, the segmentation mask, along with the raw confocal images, was imported into custom software written in MATLAB (R2015a; Mathworks, Natick, MA), with use of the image processing toolbox. The custom software performed morphological erosion on the segmentation mask to isolate individual cells, which were then each given a unique identification number, and then returned to their original size by use of morphological dilation. The boundary of the GC was then outlined manually based on the Ki67 and PD-1 expression, and the number of cells in each GC was counted. To aid comparisons between different conditions, the normalized cell count in each image was obtained by dividing the number of cells in the GC by the area (in square millimeters) of the GC.

Statistical analysis

The Mann–Whitney *U* test was used for comparisons between different groups of animals, and the Wilcoxon signed rank test was used for paired differences within the same group of animals. Correlations were assessed using the Spearman rank correlation test. Exact permutation *p* values were calculated. When small numbers of observed values yielded inadequate power for nonparametric tests, outcomes combined across groups were modeled using ANOVA after appropriate transformations to meet distributional assumptions. Numbers of cells in multiple GCs per animal were analyzed by repeated measures ANOVA, and *p* values for the multiple pairwise comparisons of the groups were corrected using the Tukey method. In all other figures, *p* values reported are not corrected for multiple comparisons. Analyses were performed using GraphPad Prism (GraphPad Software) and SAS/STAT software version 12.1 (SAS Institute, Cary, NC).

Results

$CD8^+$ and $CD4^+$ cells accumulate in LN follicular regions during the course of SIV infection

The number of $CD8^+$ and $CD4^+$ cells in LN GCs was determined immunohistochemically. Representative staining of LNs from acutely and chronically infected (LVL and HVL, viral loads shown in Fig. 1) and naive macaques is shown (Fig. 2). Eighteen GCs (7, 2, and 9, respectively) of three naive, 19 GCs (7, 8, 2, 1, and 1, respectively) of five acute, 19 GCs of four LVL (5, 6, 6, and 2, respectively) and 28 GCs (4, 5, 6, 6, and 7, respectively) of five HVL animals were analyzed. Some of the animals had less defined GCs in the tissue sections examined. We chose more defined areas for analysis, which resulted in lower GC counts in 1 of the naive and 4 of the 14 infected animals. A higher number of $CD8^+$ cells accumulated in GCs of the acutely infected compared with naive animals, with even higher accumulation in the chronically infected animals. However, no difference in the number of $CD8^+$ cells between LVL and HVL animals was observed (Fig. 3A). Compared to LN of naive macaques, more $CD4^+$ cells were seen in acutely and chronically infected animals (Fig. 3B). A positive correlation was observed between $CD8^+$ and $CD4^+$ cells/mm^2 of tissue in the acute and LVL animals (Fig. 3C, 3D), suggesting that the interaction between $CD8^+$ and $CD4^+$ starts early after exposure and continues during chronic infection in LVL but not HVL animals. Thus, $CD4^+$ cells might contribute to the proliferation of $CD8^+$ cells in the acute and LVL animals.

SIV-specific fCD8 cells accumulate in B cell follicles of SIV-infected LNs

LNs from all macaque groups (see *Materials and Methods*) were further analyzed by flow cytometry to detect SIV-specific fCD8 cells during the course of infection. The relative expression of CCR7 and CXCR5 on $CD8^+$ T cells determines their localization within LNs (38, 39). $CD8^+$ T cells expressing high CXCR5 and low CCR7, defined as fCD8 cells, are localized in B cell follicles and were gated as shown (Fig. 4A). Increased frequencies of fCD8 cells were observed in LNs of acutely and chronically infected macaques, but no difference in the level of fCD8 cells was seen between LVL and HVL groups (Fig. 4B). As CD3 cells were not stained in the immunohistochemical analysis, we examined flow cytometry data from the same LNs to determine the fraction of cells that were $CD3^+$ as well as both $CD4^+$ and $CD8^+$. The percentage of $CD3^+$ T cells in the follicular $CD4^+$ population ranged from 78.8 to 97.5%; the percentage in the follicular $CD8^+$ population ranged from 70.9 to 98.9%. The percentage of $CD4^+CD8^+$ T cells among the total follicular $CD4^+$ and $CD8^+$ cells ranged from 0.3 to 4.5%. Overall, the percentage of fCD8 cells was highest in the chronic phase of infection regardless of viral load as also observed for $CD8^+$ cells in GCs immunohistochemically (Fig. 3A).

To further investigate the expansion of fCD8 cells during the course of SIV infection, the frequency of SIV Env- and Gag-specific fCD8 cells was determined by ELISPOT assay in acutely and chronically infected macaques. Cells of both specificities were observed in infected animals, with greater levels seen in chronically infected macaques. However, no significant difference was obtained between LVL and HVL groups (Fig. 4C, 4D).

fCD8 cells in LVL animals are associated with viremia control

Granzyme B– and perforin-producing fCD8 cells were next assessed following stimulation with SIV Env and Gag peptides. Upon 6 h stimulation with peptide, the expression of CXCR5 on CD8 T cells remained unchanged (data not shown). Higher frequencies of granzyme B^+ (Fig. 4E, 4F) and perforin$^+$ (Fig. 4G, 4H) cells were observed in chronically infected animals compared with naive and acutely infected animals. Although the frequency of granzyme B^+ cells was comparable between LVL and HVL animals, fCD8 cells of LVL compared with HVL animals tended to express more granzyme B in response to Gag peptide stimulation as shown by higher MFI, suggesting a greater cytotoxic potential (Fig. 4I).

To assess the potential impact of greater Gag-specific granzyme B fCD8 cell responses in LVL macaques on viremia control, correlation analyses were performed between fCD8 cells and median plasma viremia during chronic infection (week 12 to time of necropsy) of HVL and LVL macaques and viremia at the time of necropsy of acutely infected macaques. A significant negative correlation was observed between fCD8 cells in B cell follicles and median viral load in LVL animals (Fig. 4J), but not in the other groups of animals (data not shown), suggesting that fCD8 cells might contribute to viremia control in LVL animals.

Killing capacity was next investigated as a mechanism by which fCD8 cells might contribute to viremia control. $CD8^+CXCR5^+$ and autologous $CD4^+$ cells were sorted from LNs of acute, LVL, and HVL animals. $CD4^+$ cells pulsed with SIV_{mac239} Gag peptides were used as targets and $CD8^+CXCR5^+$ fCD8 cells were used as effectors. fCD8 cells from LVL animals killed target cells more efficiently compared with those from HVL and acutely infected

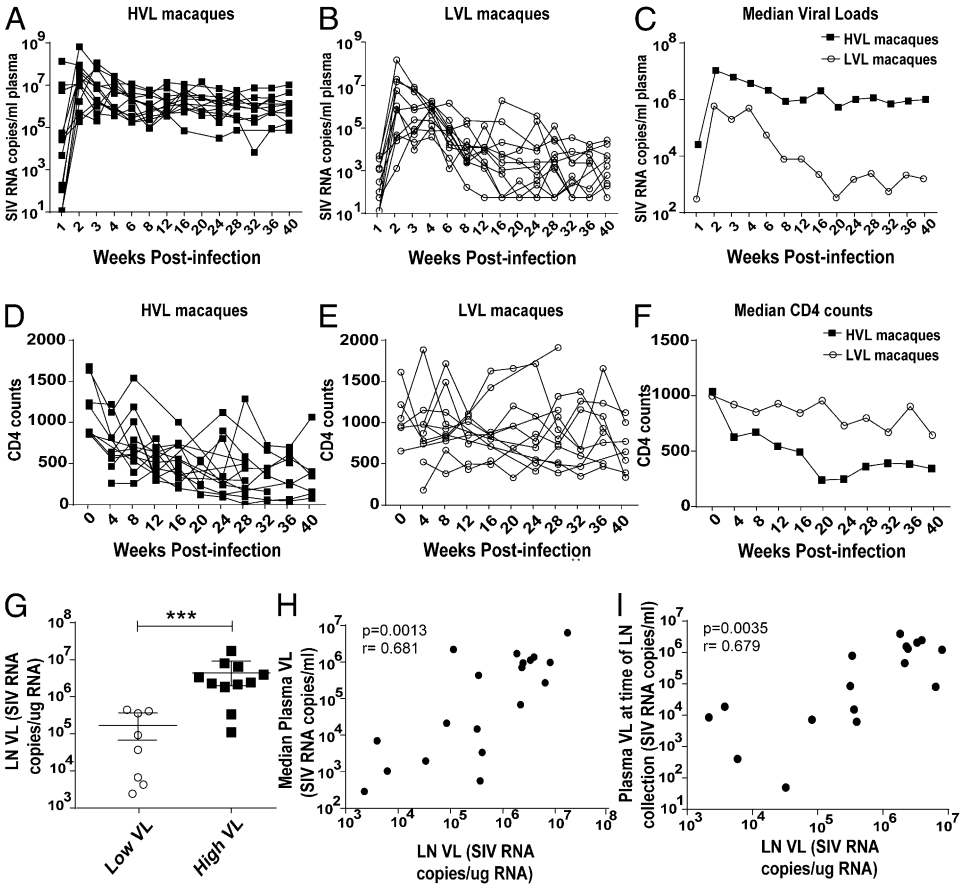

FIGURE 1. Virological and immunological status of the study animals. (**A** and **B**) Viral load of HVL and LVL animals, respectively, during the course of infection. (**C**) Median viral load of the HVL and LVL groups after infection. (**D** and **E**) CD4 counts of HVL and LVL animals, respectively, after infection. (**F**) Median CD4 counts of the HVL and LVL groups after infection. (**G**) LN viral loads of the macaques. LN cells from 8 LVL and 11 HVL macaques were available for analysis. (**H**) Correlation between LN viral loads and median plasma viral load. (**I**) Correlation between LN viral loads and plasma viral loads at the time of LN collection. Viral loads at time of LN collection for two HVL macaques were not determined. Data of (G) were analyzed by the Mann–Whitney *U* test. Data of (H) and (I) were analyzed by the Spearman correlation test. $***p < 0.001$.

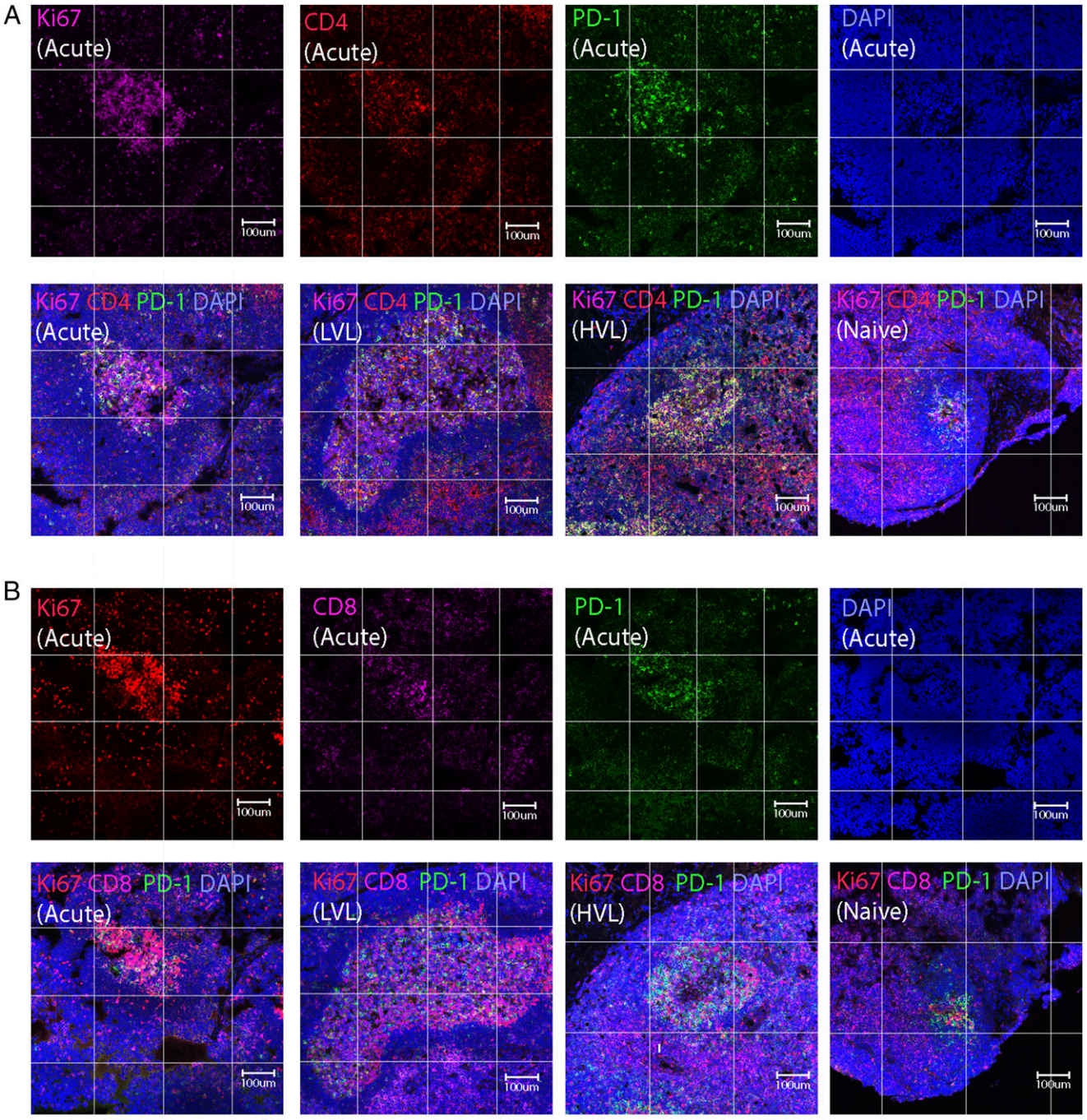

FIGURE 2. Localization of $CD4^+$ and $CD8^+$ cells in GCs of rhesus macaques. (**A**) Representative imaging of GCs for $CD4^+$ cells. Immunofluorescence staining for Ki67 (purple), CD4 (red), PD-1 (green), and nuclei (blue) of an LN section from an acutely infected macaque (top panels). Representative staining of GCs from SIV-infected macaques (acutely infected and LVL and HVL chronically infected macaques) and a naive macaque as indicated (bottom panels). (**B**) Representative imaging of GCs for $CD8^+$ cells. Immunofluorescence staining for Ki67 (red), CD8 (purple), PD-1 (green), and nuclei (blue) of an LN section from an acutely infected macaque (top panels). Representative staining of GCs from SIV-infected macaques (acutely infected and LVL and HVL chronically infected macaques) and a naive macaque as indicated (bottom panels). As the majority of GC were bigger than the single field of view, images had to be cropped from mosaic files containing spliced tile scans. Mosaic files were not processed further; visible edge artifacts for the individual images of the tile scan arising from optical aberrations and uneven illumination were not corrected. The edges of individual images combined into a mosaic file are marked by white lines.

animals (Fig. 4K), further supporting the notion that fCD8 cells contributed to control of viral load in the LVL animals.

Tfh cells are associated with fCD8 activity in SIV-infected animals

$CD8^+$ T cells control virus replication with the help of $CD4^+$ T cells, which provide IL-21, essential for maintaining $CD8^+$ T cell functionality (40, 41). The control might be compromised in the absence of $CD4^+$ T cell help (42). An increase in Tfh cells in LNs occurs following both HIV and SIV infection (11, 43); however, IL-21 production by the cells has been reported to be significantly reduced (44). Thus, we investigated LN Tfh cell–fCD8 cell interactions. Tfh cells were gated as shown (Fig. 5A) and analyzed in the four macaque groups. Overall Tfh cell

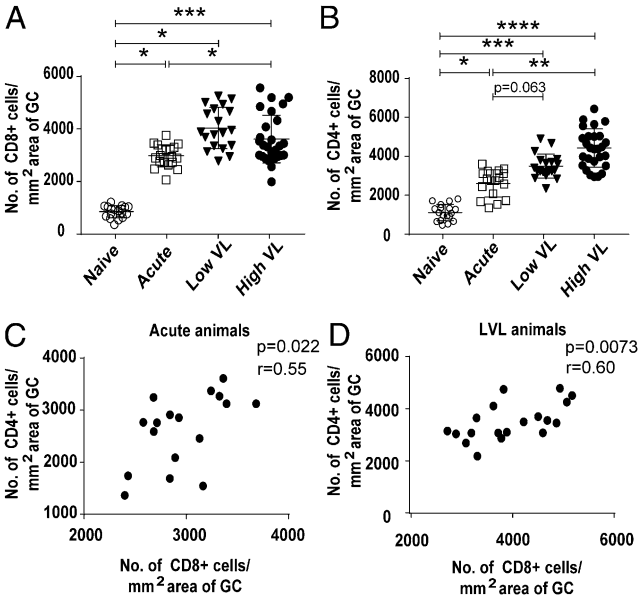

FIGURE 3. Quantitation of $CD4^+$ and $CD8^+$ cells in GCs of rhesus macaques. (**A**) Frequency of $CD8^+$ cells in GCs of naive and acutely and chronically SIV-infected macaques. (**B**) $CD4^+$ cell frequency in GCs of all groups of macaques. (**C** and **D**) Correlation between the number of $CD8^+$ and $CD4^+$ cells in acutely infected and LVL animals, respectively. Data were analyzed by repeated measures ANOVA (A and B) and the Spearman correlation test (C and D). In (A) and (B), p values for multiple pairwise comparisons of the groups were corrected using the Tukey method. Horizontal and vertical bars denote mean and SD. $^*p < 0.05$, $^{**}p < 0.01$, $^{***}p < 0.001$, $^{****}p < 0.0001$.

percentages were elevated in acutely and chronically SIV-infected animals compared with naive macaques; highest frequencies were observed in HVL animals (Fig. 5B). Comparable data were obtained on GC $CD4^+$ cells immunohistochemically (Fig. 3B). Percentages of Env- (Fig. 5C) and Gag-specific IL-21^+ Tfh cells (Fig. 5D) were highest in chronically infected macaques with no difference between HVL and LVL groups. IL-21 expression levels in response to both Env and Gag peptide stimulation, reported as MFI, although not significant tended to be higher in the LVL macaques compared with the HVL macaques (Fig. 5E, 5F). Notably in LVL macaques, but not in the other infected animals, percentages of Tfh and fCD8 cells were significantly correlated (Fig. 5G). Percentages of both Env- and Gag-specific IL-21^+ Tfh cells in the LVL group, but not in the other groups, also correlated inversely with viral load (Fig. 5H, 5I). These results are consistent with IL-21^+ Tfh cells providing help to fCD8 cells in maintaining control of viral load.

Tfreg–fCD8 cell associations suggest suppression of $CD8^+$ T cell activity in HVL SIV-infected animals

Suppressive T regulatory cells (Treg) expand in chronic infections, including HIV infection (45). They are potentially beneficial, limiting nonspecific immune activation, or detrimental, suppressing effective Ag-specific immune responses (46). Simonetta and Bourgeois (47) suggested that a balance between positive and negative Treg effects might determine disease outcome. In HIV patients reduced immune activation and LVL have been associated with increased levels of Treg (48, 49). However, in both HIV and SIV infection, Treg accumulation in lymphoid tissues has been associated with high viremia (50). Decreases in HIV-specific T cell responses in chronic infection, which contribute to viral persistence, have been associated with mucosal Treg (51). Thus, in this study we examined the effect of Tfreg on fCD8 cells and viral loads during the course of SIV infection. Tfreg were gated as shown (Fig. 6A), and comparable frequencies of Tfreg were observed among naive and acutely infected animals, with significantly elevated levels seen in chronically infected macaques, although no large difference was observed between the LVL and HVL groups (Fig. 6B).

To investigate the impact of Tfreg on disease progression, we examined relationships between frequencies of follicular T cell subpopulations determined by flow cytometry. In acutely infected macaques no significant correlation was observed between Tfreg and fCD8 cells. However, during chronic infection, Tfreg in the LVL animals exhibited a significant positive correlation with fCD8 cells (Fig. 6C), whereas a negative trend was observed in HVL animals (Fig. 6D). This suggests that although Tfreg have a beneficial effect in the LVL macaques, perhaps helping to control immune activation, they may exert suppressive effects on fCD8 cells in HVL animals. In contrast to the lack of relationship between Tfreg and fCD8 cell frequencies in the acute animals, a positive correlation was observed between Tfreg and Tfh cells in the acutely infected animals (Fig. 6E), which was lost in both groups of chronically infected macaques. Because $CD4^+$ T cells are lost during HIV/SIV infection, the absolute number of Tfreg is also important in predicting HIV infection outcomes (47). In acutely infected animals, a positive correlation was observed between the number of Tfreg and the number of Tfh cells (Fig. 6F) as well as with the number of IL-21^+ Tfh cells (Fig. 6G). These correlations were lost in the chronic phase of infection, suggesting that Tfreg play a positive role on Tfh cells in the early phase of infection.

We also investigated relationships between Tfreg and viremia levels. A strong negative correlation between Tfreg and chronic median viral load was observed in LVL animals (Fig. 6H). In view of the positive correlation between fCD8 cells and Tfreg in LVL macaques (Fig. 6C), this result is consistent with Tfreg contributing to viremia suppression. However, the percentage of Tfreg in HVL animals showed a positive trend with the median viral load (Fig. 6I), and the number of Tfreg was also positively correlated with viremia (Fig. 6J). The trend of negative correlation between fCD8 and Tfreg frequencies (Fig. 6D), together with the trend of positive correlation of Tfreg frequency with viral load and the significant association of Tfreg number with viral load in HVL macaques (Fig. 6I, 6J), suggests that Tfreg contribute to the high viremia in these animals.

Higher frequency and function of SIV-specific fCD8 cells compared with non-fCD8 cells

As antiviral $CD8^+$ T cells are important in the control of HIV/SIV replication and Tfh cells in B cell follicles are key sites of productive HIV/SIV infection (8–12, 52), we compared fCD8 cells within the B cell follicle with non-fCD8 ($CD8^+CXCR5^-$) T cells with regard to their impact on viral replication in vivo and viral load control. Higher frequencies of SIV Gag- and Env-specific fCD8 cells compared with non-fCD8 T cells were observed in SIV-infected macaques by ELISPOT assay (Fig. 7A, 7B). To investigate functionality, we examined frequencies of granzyme B^+ and perforin$^+$ cells in each compartment by flow cytometry. A previous study reported equivocal results in chronically SIV-infected macaques. Higher percentages of granzyme B^+ cells were found flow cytometrically in $CXCR5^+$ CTL, including $CCR7^-$ cells, indicating the fCD8 population, whereas perforin$^+$ cells detected by in situ tetramer staining were more prevalent in the non-fCD8 cell population (14). In the present study, flow cytometric analysis revealed higher percentages of perforin$^+$ SIV Gag- and Env-specific fCD8 cells compared with non-fCD8 cells in LNs of all SIV-infected macaques (Fig. 7C, 7D) together with

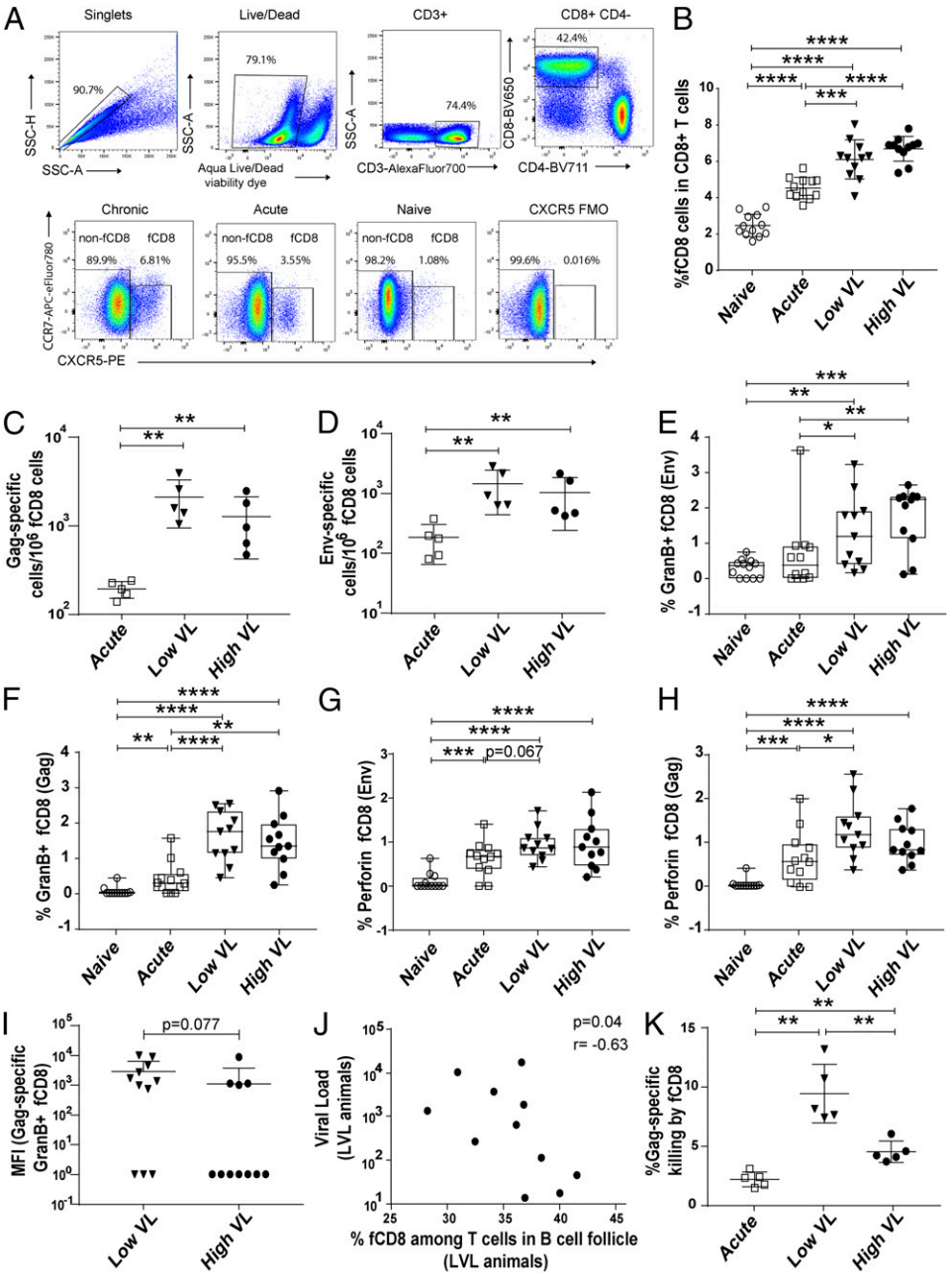

FIGURE 4. fCD8 cells during SIV infection: frequency, functionality, and association with viremia control. (**A**) Representative gating of fCD8 cells. A representative CXCR5 fluorescence-minus-one (FMO) control is shown. (**B**) Frequency of fCD8 cells in LN of naive and acutely and chronically SIV-infected macaques. (**C** and **D**) Frequency of SIV Gag- and Env-specific fCD8 cells determined by ELISPOT in acutely and chronically infected macaques. (**E**–**H**) Frequency of Env- and Gag-specific granzyme B^+ and perforin$^+$ fCD8 cells in all macaque groups following stimulation with Env and Gag peptides. (**I**) SIV Gag-specific granzyme B expression on fCD8 cells of LVL and HVL macaques, shown by MFI. Frequencies and MFI were calculated as the peptide-stimulated response minus the unstimulated response. An MFI calculated as 0 was assigned a value of 1 for plotting. (**J**) Correlation between median chronic viral load and percentage of fCD8 cells among T cells ($CD3^+CXCR5^+$) in B cell follicles of LVL macaques. (**K**) Gag-specific killing by fCD8 cells of SIV-infected macaques. Data of (B)–(I) and (K) were analyzed by the Mann–Whitney *U* test; data of (J) were analyzed by the Spearman correlation test. Horizontal and vertical bars denote mean and SD. $*p < 0.05$, $**p < 0.01$, $***p < 0.001$, $****p < 0.0001$.

greater frequencies of granzyme B^+ SIV Gag- and Env-specific fCD8 cells in LVL and HVL animals (Fig. 7E, 7F). The data suggest that SIV-specific $CD8^+$ T cells accumulate during the course of infection in B cell follicles where they are available to combat virus-infected cells.

A caveat in this regard involves the PD-1/PD-L1 pathway, which contributes to the exhaustion of HIV-specific $CD8^+$ T cells. In both HIV- (53) and SIV-specific $CD8^+$ T cells (54), PD-1 is upregulated and positively correlated with high plasma viremia and negatively correlated with $CD4^+$ T cell counts. Blocking of the PD-1/PD-L1 interaction in the SIV-macaque model has reversed exhaustion of Ag-specific $CD8^+$ T cells (54). Moreover, inhibitory PD-1 has been associated with lower functionality of $CD8^+$ T cells (55) and with decreased HIV-specific $CD8^+$ T cell proliferation (56). Whereas PD-1^+ T cells have been associated with poor functionality, these "exhausted" $CD8^+$ T cells have also been shown to play a vital role in controlling viral replication (57). In this study, we assessed PD-1 expression on fCD8 cells at different stages of SIV infection. Elevated frequencies of PD-1^+ fCD8 cells were seen in chronically infected animals, being highest in HVL animals (Fig. 8A). This result suggested that fCD8 cells of HVL macaques might have lower functionality compared with fCD8 cells of the other macaque groups. In fact, fCD8 cells of LVL macaques exhibited greater SIV-specific killing compared with both acutely infected and HVL macaques (Fig. 4K).

We further compared frequencies of PD-1^+ fCD8 cells and non-fCD8 cells. In all macaque groups, greater percentages of PD-1^+ cells were observed in the fCD8 populations (Fig. 8B). Killing assays performed using fCD8 or non-fCD8 cells as effectors with Gag peptide–pulsed autologous $CD4^+$ T targets revealed a higher percentage of killing by the fCD8 cells compared with the non-fCD8 cells, regardless of the viral load or duration of infection (Fig. 8C), and despite displaying high PD-1 frequencies, as PD-1 expression has been reported to be unreliable as a marker for immune exhaustion in chronic SIV infection (58). Higher frequencies of SIV Env- and Gag-specific non-fCD8 cells were

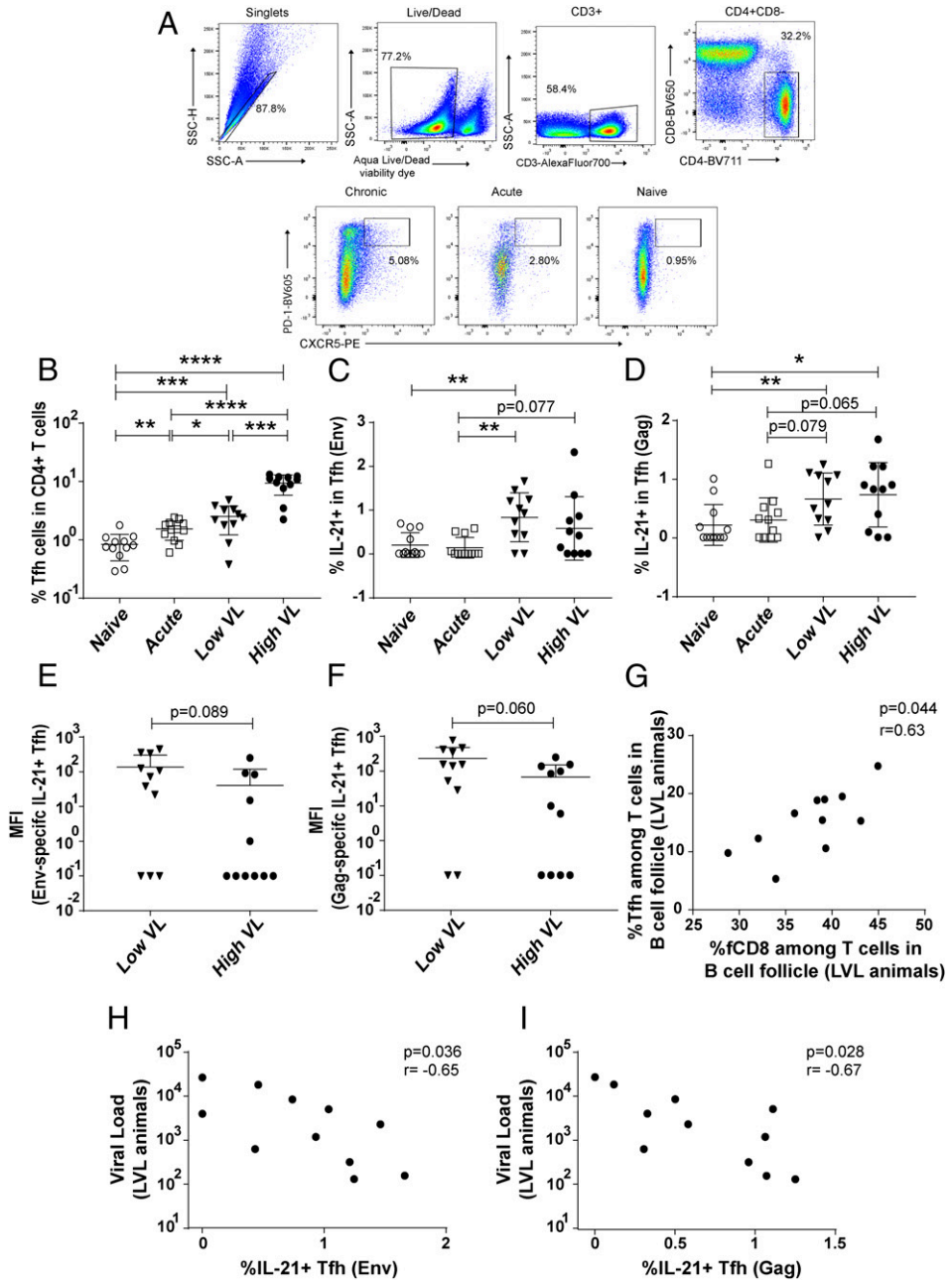

FIGURE 5. Association of Tfh and fCD8 cells in B cell follicles. (**A**) Representative gating of Tfh cells. (**B**) Frequency of Tfh cells among $CD4^+$ cells in LN of the four macaque groups. (**C** and **D**) Percentage of IL-21^+ Tfh cells in response to Gag (C) and Env (D) peptide stimulation. (**E** and **F**) IL-21 expression on Env- (E) and Gag-specific (F) Tfh cells determined by MFI in HVL and LVL animals. Frequencies and MFI were calculated as the peptide-stimulated response minus the unstimulated response. An MFI calculated as 0 was assigned a value 0.1 for plotting. (**G**) Correlation between Tfh and fCD8 cell frequencies among T cells ($CD3^+$ $CXCR5^+$) in B cell follicles of LVL macaques. (**H** and **I**) Correlation between Env- (H) and Gag-specific (I) IL-21^+ Tfh cells and median chronic viral load of LVL animals. The data of (B)–(F) were analyzed by a Mann–Whitney *U* test and (G)–(I) were analyzed by a Spearman correlation test. Horizontal and vertical bars denote mean and SD. $*p < 0.05$, $**p < 0.01$, $***p < 0.001$, $****p < 0.0001$.

observed in chronically infected animals compared with acutely infected ones (Fig. 8D, 8E), with no difference between LVL and HVL macaques and no difference in their killing capacity (Fig. 8F). Unlike fCD8 cells of LVL macaques, the frequency of non-fCD8 cells in all the LVL animals did not correlate negatively with viral load (data not shown). Therefore, killing attributed to non-fCD8 cells might not be a major contributing factor in viremia control of the LVL animals studied. Recent data following in vivo $CD8^+$ T cell depletion of SIV-infected macaques showed that whereas SIV^+ cells increased in both follicular and extrafollicular areas, the increase was ~2-fold greater in the extrafollicular region (59). The authors concluded that both follicular and extrafollicular $CD8^+$ T cells can suppress viral replication in vivo. Whether this difference from our findings results from the fact that our animals were vaccinated whereas the CD8-depleted macaques were not, or because the latter macaques had only been infected for 59 d whereas our macaques were studied after 40–50 wk of infection will require further investigation.

Discussion

Our investigation of three LN follicular T cell populations of rhesus macaques revealed correlative interactions and associations with maintenance of low viremia during SIV chronic infection. As recently reported for HIV-infected patients (31) and SIV-infected macaques (30), fCD8 cells were elevated in this study in chronically infected macaques. Although similar fCD8 cell frequencies between LVL and HVL macaques and similar frequencies of SIV Gag- and Env-specific cells and granzyme B^+ and perforin$^+$ cells were seen, granzyme B expression tended to be greater in fCD8 cells of LVL macaques. These cells also exhibited significantly greater killing compared with HVL macaques (Fig. 4K). This greater functionality suggests a mechanism by which LVL macaques maintain viremia control, supported by the negative correlation of their fCD8 cell frequency and viral load (Fig. 4J). Connick et al. (14) in an earlier study reported using a mixed model analysis that SIV-specific CTL in both follicular and extrafollicular compartments of combined LN and spleen were

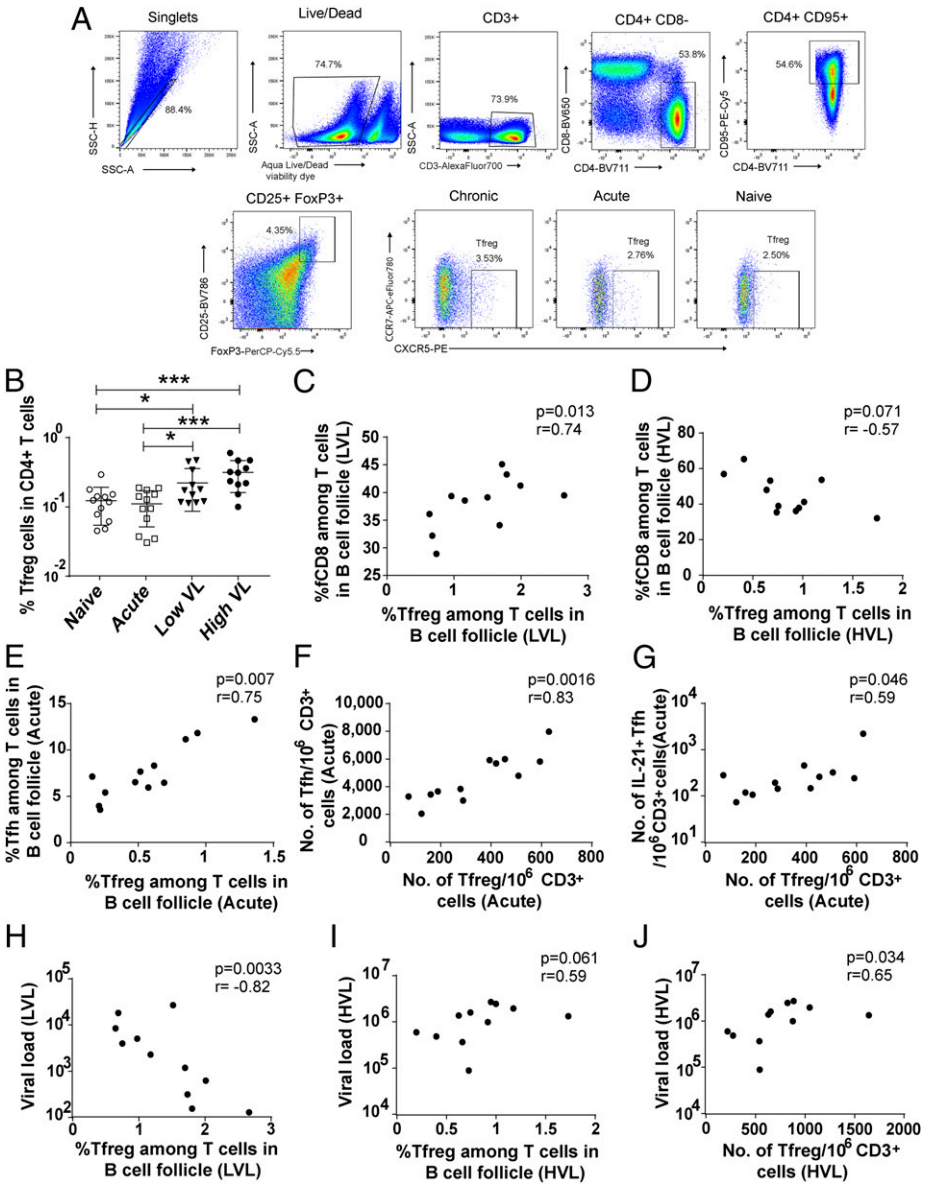

FIGURE 6. Association of Tfreg with fCD8 and Tfh cells in B cell follicles. (**A**) Representative gating of Tfreg. (**B**) Frequency of Tfreg among $CD4^+$ cells in LN of four animal groups. (**C** and **D**) Correlation between Tfreg and fCD8 cell frequencies of LVL (C) or HVL (D) animals. (**E**) Correlation between Tfreg and Tfh cell frequencies in acutely infected macaques. (**F** and **G**) Correlation between Tfreg number and Tfh cell number (F) or IL-21^+ Tfh cell number (G) in acutely infected macaques. (**H** and **I**) Correlation between the frequencies of Tfreg in LVL (H) or HVL (I) macaques and median chronic viral loads. (**J**) Correlation between Tfreg number and median chronic viral load in HVL macaques. The percentages in (C)–(E), (H), and (I) were taken among T cells ($CD3^+CXCR5^+$) in B cell follicles of the macaques. Numbers of Tfreg, Tfh cells, and IL-21^+Tfh cells in (F), (G), and (J) were normalized to 1 million $CD3^+$ cells. The data of (B) were analyzed by a Mann–Whitney *U* test; (C)–(J) were analyzed by a Spearman correlation test. Horizontal and vertical bars denote mean and SD. $*p < 0.05$, $***p < 0.001$.

inversely correlated with chronic tissue viral load of all chronically SIV-infected macaques. That study is not strictly comparable, however, to the present study. The animal populations were somewhat different, as the earlier study used macaques infected a median of 22 wk whereas our macaque samples were obtained 40–50 wk postinfection. More important differences include the fact that we correlated total fCD8 cells with plasma viral loads, whereas Connick et al. correlated dominant SIV-specific CTL in follicular and extrafollicular compartments with SIV RNA-positive cells, perhaps contributing to the different results.

Tfh cells in macaque LNs exhibited elevated frequencies associated with increasing viremia, as reported earlier (10, 12). Notably, however, Env-specific IL-21^+ Tfh cells were significantly higher in LVL macaques and tended to be higher in HVL animals (Fig. 5C) whereas Gag-specific IL-21^+ Tfh cells tended to be higher in both LVL and HVL animals compared with the acute group. Tfh and fCD8 cell frequencies were directly correlated in LVL (Fig. 5G) but not HVL macaques. Importantly, both Env- and Gag-specific IL-21^+ Tfh cells of LVL animals were significantly negatively correlated with viral loads (Fig. 5H, 5I). These results are consistent with adequate help being provided by Tfh cells to fCD8 cells in LVL but not HVL animals.

We confirmed an increased abundance of Tfreg during the course of infection (50), although no difference was observed between LVL and HVL animals. Tfreg have shown negative effects on Tfh cells in HIV and SIV infection, including inhibition of proliferation, ICOS expression, and IL-4 and IL-21 production (60). Although a positive correlation between Tfreg and Tfh cells in acutely infected animals was seen (Fig. 6E), it was lost in chronic infection. A significant positive correlation between Tfreg and fCD8 cells in the LVL animals (Fig. 6C), as well as a negative correlation between Tfreg and viral load (Fig. 6H), suggested that Tfreg positively impact fCD8 cells, which in turn control viremia. Importantly, in chronic viral infections, Treg have been shown to suppress $CD8^+$ T cell activity in a contact-dependent manner (61). Moreover, in situ staining of LN tissue sections for SIV-specific $CD8^+$ T cells and $Foxp3^+$ Tregs revealed significant numbers of these cells in direct contact (59), further suggesting cell interactions. Strikingly, however, a significant negative correlation was seen between Tfreg and fCD8 cell frequencies in HVL macaques (Fig. 6D). Additionally, a strong positive trend was seen between Tfreg frequency in HVL animals and their viral loads (Fig. 6I), along with a significant positive correlation between Tfreg number and viral load (Fig. 6J). These data suggest suppression of fCD8

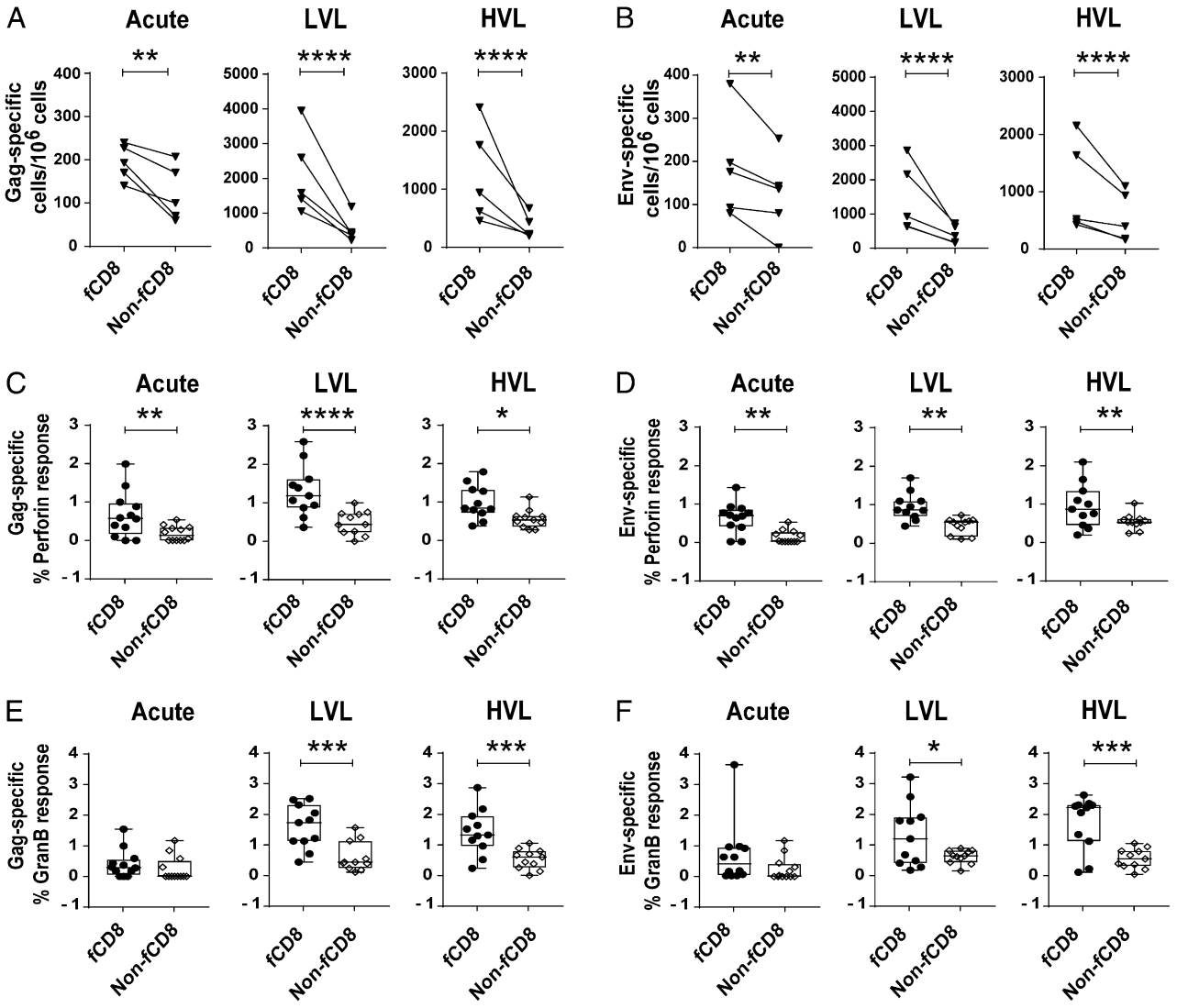

FIGURE 7. Comparison of SIV-specific frequency and cytokine-producing cells in fCD8 and non-fCD8 cells. (**A** and **B**) Frequency of SIV Gag- and Env-specific fCD8 and non-fCD8 cells in LN of SIV-infected macaques. (**C**–**F**) Percentage of SIV-specific perforin$^+$ (C and D) and granzyme B$^+$ (E and F) fCD8 and non-fCD8 cells in response to Gag (C and E) or Env (D and F) peptide stimulation. The data of (A)–(F) were analyzed with ANOVA. Horizontal and vertical bars denote mean and SD. *$p < 0.05$, **$p < 0.01$, ***$p < 0.001$, ****$p < 0.0001$.

cells by Tfreg might contribute to the loss of viremia control in the HVL animals.

Although we focused on CD4$^+$ Tfreg in the present study, CD8$^+$ Tfreg have been shown to make up most of the CD8 T cells within follicles of both humans and macaques (62) and to impair both Tfh and GC B cell responses. As they have been characterized as having limited cytotoxic potential, they could be critical in maintaining persistent HIV and SIV infection of lymphoid follicles.

Overall, these results illustrate the complexity of cellular activities within LN follicles, and they indicate that assessment of a single T cell population and associated molecular mechanisms will be insufficient to fully understand pathogen control. Detection of fCD8 cells in B cell follicles of secondary lymphoid organs in humans, as well as in murine and macaque models (14, 16, 17, 27–31), suggested that fCD8 cells enter B cell follicles and contribute to eradication of infected cells. Although HIV-specific killing in vitro was reported in the presence of bispecific Ab (31), to our knowledge, this is the first report showing SIV peptide–specific killing of target cells by fCD8 cells isolated from LN. Although fCD8 cells of LVL animals had higher killing capacity and were negatively correlated with viremia, fCD8 cells were also detected in HVL animals. Their higher expression of PD-1 is not necessarily firm evidence of immune exhaustion (58), and other mechanisms may contribute to their impaired viremia control. Although Tfh cell frequency was highest in HVL animals, these cells tended to have lower frequencies and/or expression of IL-21, suggesting dysfunction and diminished support of fCD8 cells. In fact, unlike LVL animals, the percentage of IL-21$^+$ Tfh cells in HVL animals did not correlate with reduced viral load or fCD8 cell frequency. Additionally, a negative impact of Tfreg on fCD8 cells, suggested by the negative correlation in HVL macaques (Fig. 6D), is consistent with lower viral control by fCD8 cells in these animals.

The frequencies of SIV Env- and Gag-specific fCD8 cells compared with non-fCD8 cells were higher in LNs of infected animals (Fig. 7A, 7B). Furthermore, the frequencies of SIV-specific granzyme B$^+$ and perforin$^+$ cells were higher in fCD8 cells compared with non-fCD8 populations (Fig. 7C, 7D). These data explain the higher SIV-specific killing by fCD8 cells compared with non-fCD8 cells, and they are consistent with results obtained in the LCMV mouse model, where fCD8

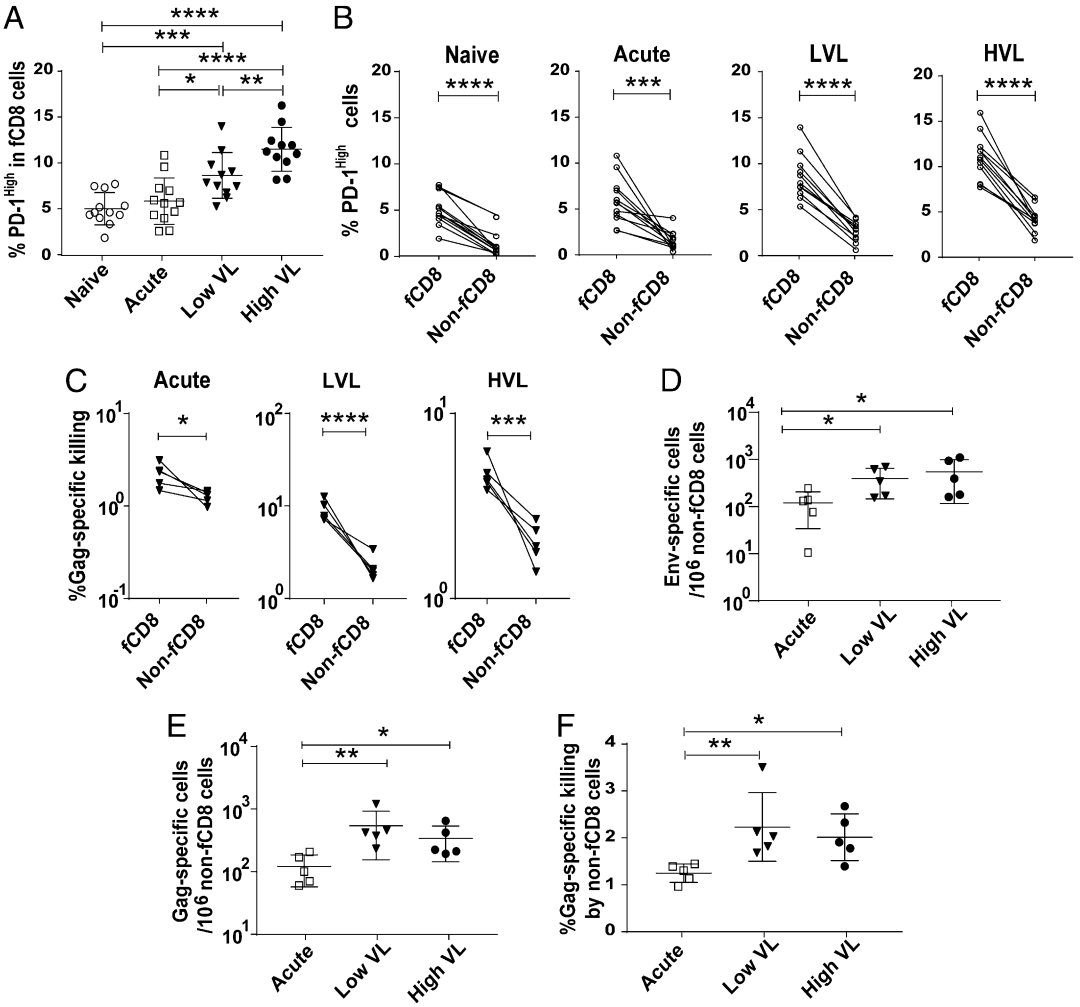

FIGURE 8. Comparison of phenotypic and functional properties of fCD8 and non-fCD8 cells. (**A**) Percentage of PD-1^{high} fCD8 cells among four groups of macaques. (**B**) PD-1^{high} fCD8 and non-fCD8 cells in naive and SIV-infected animals. (**C**) Specific killing by fCD8 and non-fCD8 cells of SIV-infected macaques. (**D** and **E**) Frequencies of SIV Env- and Gag-specific non-fCD8 cells in acutely and chronically SIV infected macaques, determined by ELISPOT. (**F**) Gag-specific killing by non-fCD8 cells among acutely and chronically infected macaques. The data of (A) and (D)–(F) were analyzed by a Mann–Whitney *U* test, and (B) and (C) were analyzed by ANOVA. Horizontal and vertical bars denote mean and SD. $*p < 0.05$, $**p < 0.01$, $***p < 0.001$, $****p < 0.0001$.

cells exhibited more potent cytotoxicity than does the $CXCR5^-$ subset (29). SIV-specific killing in non-fCD8 cell populations was higher in the chronic phase compared with the acute phase, but no difference in killing was observed between LVL and HVL animals. Moreover, the frequency of SIV-specific non-fCD8 cells did not correlate with viral loads, suggesting that the activity of fCD8 cells might be more important for viremia control.

Overall, our results suggest that elimination of virus-infected cells in B cell follicles does not only depend on the cytotoxicity of fCD8 cells but also interaction of fCD8 cells with other T follicular cells, including Tfh cells and Tfreg. Note that all but one in each group of the chronically infected HVL and LVL macaques in our study had been previously vaccinated, so our results cannot be generalized to what might occur in natural infection. Whether the vaccination regimen had long-term effects on follicular T cell populations in the macaques 40–50 wk postinfection remains to be determined. A recent abstract reported that a DNA/MVA SHIV vaccine regimen elicited SHIV-specific $CXCR5^+CD8^+$ T cells in the blood of rhesus macaques and were enhanced when the regimen was adjuvanted with CD40L (63). The frequency of these cells was inversely correlated with peak viral load following SHIV infection. Future studies will be critical in determining whether immunization can induce potent fCD8 cells leading to protection or enhanced control of viremia. In addition to prophylactic vaccines, further understanding of how to direct the differentiation and function of fCD8 and other follicular T cell populations might lead to the design of new strategies for eliminating HIV/SIV reservoirs.

Acknowledgments

We thank the staffs at the National Cancer Institute animal facility and Advanced BioScience Laboratories, Inc., and Tanya Hoang and Sophia Brown (Vaccine Branch, National Cancer Institute) for laboratory and flow cytometry support. PE anti-CXCR5 was obtained through the National Institutes of Health Nonhuman Primate Reagent Resource. The following reagents were obtained through the AIDS Research and Reference Reagent Program (Division of AIDS, National Institute of Allergy and Infectious Diseases, National Institutes of Health): SIV_{mac239} Env and SIV_{mac239} Gag peptides (complete sets).

Disclosures

The authors have no financial conflicts of interest.

References

1. Centers for Disease Control (CDC). 1982. Persistent, generalized lymphadenopathy among homosexual males. *MMWR Morb. Mortal. Wkly. Rep.* 31: 249–251.
2. Ioachim, H. L., C. W. Lerner, and M. L. Tapper. 1983. Lymphadenopathies in homosexual men. Relationships with the acquired immune deficiency syndrome. *JAMA* 250: 1306–1309.
3. Tenner-Racz, K., P. Racz, M. Bofill, A. Schulz-Meyer, M. Dietrich, P. Kern, J. Weber, A. J. Pinching, F. Veronese-Dimarzo, M. Popovic, et al. 1986. HTLV-III/LAV viral antigens in lymph nodes of homosexual men with persistent generalized lymphadenopathy and AIDS. *Am. J. Pathol.* 123: 9–15.
4. Biberfeld, P., K. J. Chayt, L. M. Marselle, G. Biberfeld, R. C. Gallo, and M. E. Harper. 1986. HTLV-III expression in infected lymph nodes and relevance to pathogenesis of lymphadenopathy. *Am. J. Pathol.* 125: 436–442.
5. Ringler, D. J., M. S. Wyand, D. G. Walsh, J. J. MacKey, L. V. Chalifoux, M. Popovic, A. A. Minassian, P. K. Sehgal, M. D. Daniel, R. C. Desrosiers, and N. W. King. 1989. Cellular localization of simian immunodeficiency virus in lymphoid tissues. I. Immunohistochemistry and electron microscopy. *Am. J. Pathol.* 134: 373–383.
6. Breitfeld, D., L. Ohl, E. Kremmer, J. Ellwart, F. Sallusto, M. Lipp, and R. Förster. 2000. Follicular B helper T cells express CXC chemokine receptor 5, localize to B cell follicles, and support immunoglobulin production. *J. Exp. Med.* 192: 1545–1552.
7. Schaerli, P., K. Willimann, A. B. Lang, M. Lipp, P. Loetscher, and B. Moser. 2000. CXC chemokine receptor 5 expression defines follicular homing T cells with B cell helper function. *J. Exp. Med.* 192: 1553–1562.
8. McIlroy, D., B. Autran, R. Cheynier, S. Wain-Hobson, J.-P. Clauvel, E. Oksenhendler, P. Debré, and A. Hosmalin. 1995. Infection frequency of dendritic cells and $CD4^+$ T lymphocytes in spleens of human immunodeficiency virus-positive patients. *J. Virol.* 69: 4737–4745.
9. Haase, A. T. 1999. Population biology of HIV-1 infection: viral and $CD4^+$ T cell demographics and dynamics in lymphatic tissues. *Annu. Rev. Immunol.* 17: 625–656.
10. Perreau, M., A. L. Savoye, E. De Crignis, J. M. Corpataux, R. Cubas, E. K. Haddad, L. De Leval, C. Graziosi, and G. Pantaleo. 2013. Follicular helper T cells serve as the major CD4 T cell compartment for HIV-1 infection, replication, and production. *J. Exp. Med.* 210: 143–156.
11. Petrovas, C., T. Yamamoto, M. Y. Gerner, K. L. Boswell, K. Wloka, E. C. Smith, D. R. Ambrozak, N. G. Sandler, K. J. Timmer, X. Sun, et al. 2012. CD4 T follicular helper cell dynamics during SIV infection. *J. Clin. Invest.* 122: 3281–3294.
12. Xu, H., X. Wang, N. Malam, P. P. Aye, X. Alvarez, A. A. Lackner, and R. S. Veazey. 2015. Persistent simian immunodeficiency virus infection drives differentiation, aberrant accumulation, and latent infection of germinal center follicular T helper cells. *J. Virol.* 90: 1578–1587.
13. Banga, R., F. A. Procopio, A. Noto, G. Pollakis, M. Cavassini, K. Ohmiti, J. M. Corpataux, L. de Leval, G. Pantaleo, and M. Perreau. 2016. PD-1^+ and follicular helper T cells are responsible for persistent HIV-1 transcription in treated aviremic individuals. *Nat. Med.* 22: 754–761.
14. Connick, E., J. M. Folkvord, K. T. Lind, E. G. Rakasz, B. Miles, N. A. Wilson, M. L. Santiago, K. Schmitt, E. B. Stephens, H. O. Kim, et al. 2014. Compartmentalization of simian immunodeficiency virus replication within secondary lymphoid tissues of rhesus macaques is linked to disease stage and inversely related to localization of virus-specific CTL. *J. Immunol.* 193: 5613–5625.
15. Fukazawa, Y., R. Lum, A. A. Okoye, H. Park, K. Matsuda, J. Y. Bae, S. I. Hagen, R. Shoemaker, C. Deleage, C. Lucero, et al. 2015. B cell follicle sanctuary permits persistent productive simian immunodeficiency virus infection in elite controllers. *Nat. Med.* 21: 132–139.
16. Connick, E., T. Mattila, J. M. Folkvord, R. Schlichtemeier, A. L. Meditz, M. G. Ray, M. D. McCarter, S. Mawhinney, A. Hage, C. White, and P. J. Skinner. 2007. CTL fail to accumulate at sites of HIV-1 replication in lymphoid tissue. *J. Immunol.* 178: 6975–6983.
17. Folkvord, J. M., C. Armon, and E. Connick. 2005. Lymphoid follicles are sites of heightened human immunodeficiency virus type 1 (HIV-1) replication and reduced antiretroviral effector mechanisms. *AIDS Res. Hum. Retroviruses* 21: 363–370.
18. Edwards, B. H., A. Bansal, S. Sabbaj, J. Bakari, M. J. Mulligan, and P. A. Goepfert. 2002. Magnitude of functional $CD8^+$ T-cell responses to the gag protein of human immunodeficiency virus type 1 correlates inversely with viral load in plasma. *J. Virol.* 76: 2298–2305.
19. Kiepiela, P., K. Ngumbela, C. Thobakgale, D. Ramduth, I. Honeyborne, E. Moodley, S. Reddy, C. de Pierres, Z. Mncube, N. Mkhwanazi, et al. 2007. $CD8^+$ T-cell responses to different HIV proteins have discordant associations with viral load. *Nat. Med.* 13: 46–53 .
20. Jin, X., D. E. Bauer, S. E. Tuttleton, S. Lewin, A. Gettie, J. Blanchard, C. E. Irwin, J. T. Safrit, J. Mittler, L. Weinberger, et al. 1999. Dramatic rise in plasma viremia after $CD8^+$ T cell depletion in simian immunodeficiency virus-infected macaques. *J. Exp. Med.* 189: 991–998.
21. Schmitz, J. E., M. J. Kuroda, S. Santra, V. G. Sasseville, M. A. Simon, M. A. Lifton, P. Racz, K. Tenner-Racz, M. Dalesandro, B. J. Scallon, et al. 1999. Control of viremia in simian immunodeficiency virus infection by $CD8^+$ lymphocytes. *Science* 283: 857–860.
22. Devergne, O., M. Peuchmaur, M.-C. Crevon, J. A. Trapani, M.-C. Maillot, P. Galanaud, and D. Emilie. 1991. Activation of cytotoxic cells in hyperplastic lymph nodes from HIV-infected patients. *AIDS* 5: 1071–1079.
23. Tenner-Racz, K., P. Racz, C. Thomé, C. G. Meyer, P. J. Anderson, S. F. Schlossman, and N. L. Letvin. 1993. Cytotoxic effector cell granules recognized by the monoclonal antibody TIA-1 are present in $CD8^+$ lymphocytes in lymph nodes of human immunodeficiency virus-1-infected patients. *Am. J. Pathol.* 142: 1750–1758.
24. Reimann, K. A., G. B. Snyder, L. V. Chalifoux, B. C. D. Waite, M. D. Miller, H. Yamamoto, O. Spertini, and N. L. Letvin. 1991. An activated $CD8^+$ lymphocyte appears in lymph nodes of rhesus monkeys early after infection with simian immunodeficiency virus. *J. Clin. Invest.* 88: 1113–1120.
25. Rosenberg, Y. J., M. H. Kosco, M. G. Lewis, E. C. Leon, J. J. Greenhouse, K. E. Bieg, G. A. Eddy, and P. M. Zack. 1993. Changes in follicular dendritic cell and $CD8^+$ cell function in macaque lymph nodes following infection with SIV251. *Adv. Exp. Med. Biol.* 329: 417–423.
26. Schwartz, C., S. Bouchat, C. Marban, V. Gautier, C. Van Lint, O. Rohr, and V. Le Douce. 2017. On the way to find a cure: purging latent HIV-1 reservoirs. *Biochem. Pharmacol.* 146: 10–22.
27. Quigley, M. F., V. D. Gonzalez, A. Granath, J. Andersson, and J. K. Sandberg. 2007. $CXCR5^+$ $CCR7^-$ CD8 T cells are early effector memory cells that infiltrate tonsil B cell follicles. *Eur. J. Immunol.* 37: 3352–3362.
28. Leong, Y. A., Y. Chen, H. S. Ong, D. Wu, K. Man, C. Deleage, M. Minnich, B. J. Meckiff, Y. Wei, Z. Hou, et al. 2016. $CXCR5^+$ follicular cytotoxic T cells control viral infection in B cell follicles. *Nat. Immunol.* 17: 1187–1196.
29. He, R., S. Hou, C. Liu, A. Zhang, Q. Bai, M. Han, Y. Yang, G. Wei, T. Shen, X. Yang, et al. 2016. Follicular CXCR5-expressing $CD8^+$ T cells curtail chronic viral infection. [Published erratum appears in 2016 *Nature* 540: 470] *Nature* 537: 412–428.
30. Mylvaganam, G. H., D. Rios, H. M. Abdelaal, S. Iyer, G. Tharp, M. Mavinger, S. Hicks, A. Chahroudi, R. Ahmed, S. E. Bosinger, et al. 2017. Dynamics of SIV-specific $CXCR5^+$ CD8 T cells during chronic SIV infection. [Published erratum appears in 2017 *Proc. Natl. Acad. Sci. USA* 114: E3366.] *Proc. Natl. Acad. Sci. USA* 114: 1976–1981.
31. Petrovas, C., S. Ferrando-Martinez, M. Y. Gerner, J. P. Casazza, A. Pegu, C. Deleage, A. Cooper, J. Hataye, S. Andrews, D. Ambrozak, et al. 2017. Follicular CD8 T cells accumulate in HIV infection and can kill infected cells in vitro via bispecific antibodies. *Sci. Transl. Med.* 9: eaag2285.
32. Tuero, I., V. Mohanram, T. Musich, L. Miller, D. A. Vargas-Inchaustegui, T. Demberg, D. Venzon, I. Kalisz, V. S. Kalyanaraman, R. Pal, et al. 2015. Mucosal B cells are associated with delayed SIV acquisition in vaccinated female but not male rhesus macaques following SIV_{mac251} rectal challenge. *PLoS Pathog.* 11: e1005101.
33. Vargas-Inchaustegui, D. A., S. Helmold Hait, H. K. Chung, J. Narola, T. Hoang, and M. Robert-Guroff. 2017. Phenotypic and functional characterization of circulatory, splenic, and hepatic NK cells in simian immunodeficiency virus-controlling macaques. *J. Immunol.* 199: 3202–3211.
34. Vargas-Inchaustegui, D. A., O. Ying, T. Demberg, and M. Robert-Guroff. 2016. Evaluation of functional NK cell responses in vaccinated and SIV-infected rhesus macaques. *Front. Immunol.* 7: 340.
35. Allen, C. D., T. Okada, and J. G. Cyster. 2007. Germinal-center organization and cellular dynamics. *Immunity* 27: 190–202.
36. Vargas-Inchaustegui, D. A., A. Demers, J. M. Shaw, G. Kang, D. Ball, I. Tuero, T. Musich, V. Mohanram, T. Demberg, T. S. Karpova, et al. 2016. Vaccine induction of lymph node-resident simian immunodeficiency virus Env-specific T follicular helper cells in rhesus macaques. *J. Immunol.* 196: 1700–1710.
37. Sommer, C., C. Straehle, U. Koethe, and F. A. Hamprecht. 2011. ilastik: interactive learning and segmentation toolkit. In *8th IEEE International Symposium on Biomedical Imaging (ISBI 2011), March 30, 2011*. IEEE, Piscataway, NJ, p. 230–233.
38. Hardtke, S., L. Ohl, and R. Förster. 2005. Balanced expression of CXCR5 and CCR7 on follicular T helper cells determines their transient positioning to lymph node follicles and is essential for efficient B-cell help. *Blood* 106: 1924–1931.
39. Haynes, N. M., C. D. Allen, R. Lesley, K. M. Ansel, N. Killeen, and J. G. Cyster. 2007. Role of CXCR5 and CCR7 in follicular Th cell positioning and appearance of a programmed cell death gene-1^{high} germinal center-associated subpopulation. *J. Immunol.* 179: 5099–5108.
40. Elsaesser, H., K. Sauer, and D. G. Brooks. 2009. IL-21 is required to control chronic viral infection. *Science* 324: 1569–1572.
41. Yi, J. S., M. Du, and A. J. Zajac. 2009. A vital role for interleukin-21 in the control of a chronic viral infection. *Science* 324: 1572–1576.
42. Janssen, E. M., E. E. Lemmens, T. Wolfe, U. Christen, M. G. von Herrath, and S. P. Schoenberger. 2003. $CD4^+$ T cells are required for secondary expansion and memory in $CD8^+$ T lymphocytes. *Nature* 421: 852–856.
43. Lindqvist, M., J. van Lunzen, D. Z. Soghoian, B. D. Kuhl, S. Ranasinghe, G. Kranias, M. D. Flanders, S. Cutler, N. Yudanin, M. I. Muller, et al. 2012. Expansion of HIV-specific T follicular helper cells in chronic HIV infection. *J. Clin. Invest.* 122: 3271–3280.
44. Cubas, R. A., J. C. Mudd, A. L. Savoye, M. Perreau, J. van Grevenynghe, T. Metcalf, E. Connick, A. Meditz, G. J. Freeman, G. Abesada-Terk, Jr, et al. 2013. Inadequate T follicular cell help impairs B cell immunity during HIV infection. *Nat. Med.* 19: 494–499.
45. Aandahl, E. M., J. Michaëlsson, W. J. Moretto, F. M. Hecht, and D. F. Nixon. 2004. Human $CD4^+$ $CD25^+$ regulatory T cells control T-cell responses to human immunodeficiency virus and cytomegalovirus antigens. *J. Virol.* 78: 2454–2459.
46. Chevalier, M. F., and L. Weiss. 2013. The split personality of regulatory T cells in HIV infection. *Blood* 121: 29–37.
47. Simonetta, F., and C. Bourgeois. 2013. $CD4^+FOXP3^+$ regulatory T-cell subsets in human immunodeficiency virus infection. *Front. Immunol.* 4: 215.
48. Eggena, M. P., B. Barugahare, N. Jones, M. Okello, S. Mutalya, C. Kityo, P. Mugyenyi, and H. Cao. 2005. Depletion of regulatory T cells in HIV infection is associated with immune activation. *J. Immunol.* 174: 4407–4414.

49. Prendergast, A., J. G. Prado, Y. H. Kang, F. Chen, L. A. Riddell, G. Luzzi, P. Goulder, and P. Klenerman. 2010. HIV-1 infection is characterized by profound depletion of CD161$^+$ Th17 cells and gradual decline in regulatory T cells. *AIDS* 24: 491–502.
50. Nilsson, J., A. Boasso, P. A. Velilla, R. Zhang, M. Vaccari, G. Franchini, G. M. Shearer, J. Andersson, and C. Chougnet. 2006. HIV-1-driven regulatory T-cell accumulation in lymphoid tissues is associated with disease progression in HIV/AIDS. *Blood* 108: 3808–3817.
51. Shaw, J. M., P. W. Hunt, J. W. Critchfield, D. H. McConnell, J. C. Garcia, R. B. Pollard, M. Somsouk, S. G. Deeks, and B. L. Shacklett. 2011. Increased frequency of regulatory T cells accompanies increased immune activation in rectal mucosae of HIV-positive noncontrollers. *J. Virol.* 85: 11422–11434.
52. Mylvaganam, G. H., V. Velu, J. J. Hong, S. Sadagopal, S. Kwa, R. Basu, B. Lawson, F. Villinger, and R. R. Amara. 2014. Diminished viral control during simian immunodeficiency virus infection is associated with aberrant PD-1^{hi} CD4 T cell enrichment in the lymphoid follicles of the rectal mucosa. *J. Immunol.* 193: 4527–4536.
53. Day, C. L., D. E. Kaufmann, P. Kiepiela, J. A. Brown, E. S. Moodley, S. Reddy, E. W. Mackey, J. D. Miller, A. J. Leslie, C. DePierres, et al. 2006. PD-1 expression on HIV-specific T cells is associated with T-cell exhaustion and disease progression. *Nature* 443: 350–354.
54. Velu, V., K. Titanji, B. Zhu, S. Husain, A. Pladevega, L. Lai, T. H. Vanderford, L. Chennareddi, G. Silvestri, G. J. Freeman, et al. 2009. Enhancing SIV-specific immunity in vivo by PD-1 blockade. *Nature* 458: 206–210.
55. Golden-Mason, L., B. Palmer, J. Klarquist, J. A. Mengshol, N. Castelblanco, and H. R. Rosen. 2007. Upregulation of PD-1 expression on circulating and intrahepatic hepatitis C virus-specific CD8$^+$ T cells associated with reversible immune dysfunction. *J. Virol.* 81: 9249–9258.
56. Trautmann, L., L. Janbazian, N. Chomont, E. A. Said, S. Gimmig, B. Bessette, M. R. Boulassel, E. Delwart, H. Sepulveda, R. S. Balderas, et al. 2006. Upregulation of PD-1 expression on HIV-specific CD8$^+$ T cells leads to reversible immune dysfunction. [Published erratum appears in 2006 *Nat. Med.* 12: 1329.] *Nat. Med.* 12: 1198–1202.
57. Speiser, D. E., D. T. Utzschneider, S. G. Oberle, C. Münz, P. Romero, and D. Zehn. 2014. T cell differentiation in chronic infection and cancer: functional adaptation or exhaustion? *Nat. Rev. Immunol.* 14: 768–774.
58. Hong, J. J., P. K. Amancha, K. Rogers, A. A. Ansari, and F. Villinger. 2013. Re-evaluation of PD-1 expression by T cells as a marker for immune exhaustion during SIV infection. *PLoS One* 8: e60186.
59. Li, S., J. M. Folkvord, E. G. Rakasz, H. M. Abdelaal, R. K. Wagstaff, K. J. Kovacs, H. O. Kim, R. Sawahata, S. MaWhinney, D. Masopust, et al. 2016. Simian immunodeficiency virus-producing cells in follicles are partially suppressed by CD8$^+$ cells in vivo. *J. Virol.* 90: 11168–11180.
60. Miles, B., S. M. Miller, J. M. Folkvord, A. Kimball, M. Chamanian, A. L. Meditz, T. Arends, M. D. McCarter, D. N. Levy, E. G. Rakasz, et al. 2015. Follicular regulatory T cells impair follicular T helper cells in HIV and SIV infection. *Nat. Commun.* 6: 8608.
61. Park, H. J., J. S. Park, Y. H. Jeong, J. Son, Y. H. Ban, B. H. Lee, L. Chen, J. Chang, D. H. Chung, I. Choi, and S. J. Ha. 2015. PD-1 upregulated on regulatory T cells during chronic virus infection enhances the suppression of CD8$^+$ T cell immune response via the interaction with PD-L1 expressed on CD8$^+$ T cells. *J. Immunol.* 194: 5801–5811.
62. Miles, B., S. M. Miller, J. M. Folkvord, D. N. Levy, E. G. Rakasz, P. J. Skinner, and E. Connick. 2016. Follicular regulatory CD8 T cells impair the germinal center response in SIV and ex vivo HIV infection. *PLoS Pathog.* 12: e1005924.
63. Velu, V., T. Styles, P. B. J. Reddy, S. Hicks, S. Gangadhara, and R. R. Amara. 2017. Induction of CXCR5$^+$ follicular CD8 T cells by CD40L adjuvanted DNA/MVA vaccination is associated with enhanced control of pathogenic SHIV infection. *J. Immunol.* 198 (1 Suppl.): 73.14.